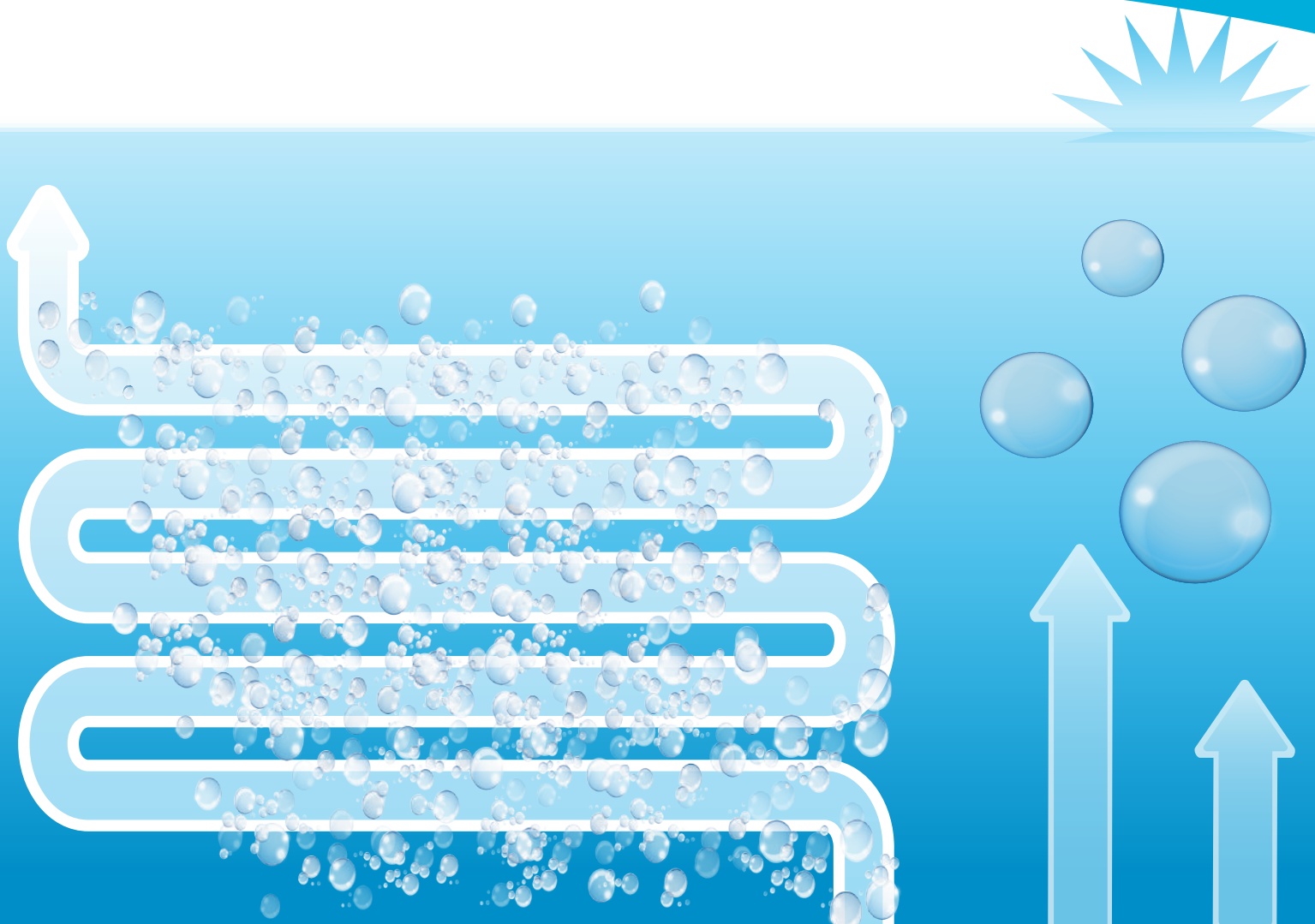




MICRO BUBBLE GENERATOR

Principle And Applications Of Microbubble
And Nanobubble Technology
For Water Treatment



Principle And Applications Of Microbubble And Nanobubble Technology For Water Treatment

Ashutosh Agarwal, Wun Jern Ng, Yu Liu*

doi:10.1016/j.chemosphere.2011.05.054

[Get rights and content](#)

Abstract

In recent years, microbubble and nanobubble technologies have drawn great attention due to their wide applications in many fields of science and technology, such as water treatment, biomedical engineering, and nanomaterials. In this paper, we discuss the physics, methods of generation of microbubbles (MBs) and nanobubbles (NBs), while production of free radicals from MBs and NBs are reviewed with the focuses on degradation of toxic compounds, water disinfection, and cleaning/defouling of solid surfaces including membrane. Due to their ability to produce free radicals, it can be expected that the future prospects of MBs and NBs will be immense and yet more to be explored.

Highlights

- We review the potential application of micro and nanobubbles for water treatment.
- The physics and generation methods of micro and nanobubbles are discussed. ► The production of free radicals by the collapse of microbubbles is reviewed. ► Micro and nanobubbles for water disinfection, degradation of organic compounds and defouling are highlighted. ► Micro and nanobubbles technology appears to be a cost-effective and environmentally friendly approach for water treatment.

Keywords

Microbubbles; Nanobubbles; Free radicals; Degradation; Disinfection; Defouling

1. Microbubbles and nanobubbles

Microbubbles (MBs) and nanobubbles (NBs) are tiny bubbles with a respective diameter of 10–50 μm and <200 nm, and have been explored for various applications. The existence of NBs as stable entity has been debated for a long while due to some thermodynamic considerations. For example, the total free energy of the system has been supposed to increase along with the formation of NBs unless the surface was extremely rough. However, high Laplace pressure inside NBs would likely cause them to dissolve into solution quickly (Ljunggren and Eriksson, 1997 and Eriksson and Ljunggren, 1999).

Fig. 1 shows the key differences among macrobubbles, MBs and NBs. MBs tend to gradually decrease in size and subsequently collapse due to long stagnation and dissolution of interior gases into the surrounding water, whereas NBs remains as such for months and do not burst out at once (Takahashi, 2009). It has been revealed that the interface of NBs consists of hard hydrogen bonds similar to those found in ice and gas hydrates. This in turn leads to reduced diffusivity of NBs that helps to maintain adequate kinetic balance of NBs against high internal pressure.

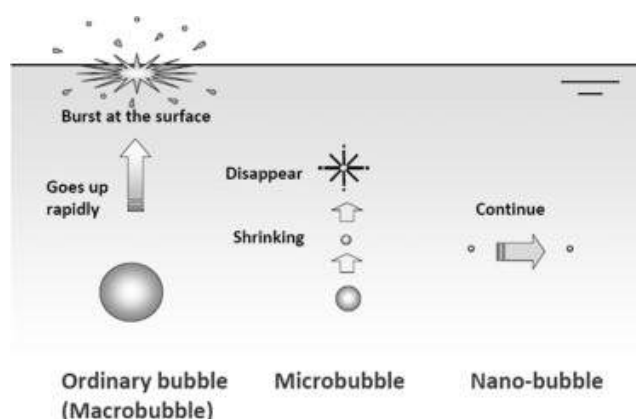


Fig. 1. Schematic diagram showing macro, micro and nanobubbles (Takahashi et al., 2007b).

caption
Figure options

2. Physics of micro and nanobubbles

The existence of NBs at the liquid–solid interface has been demonstrated by various techniques, e.g. atomic force microscopy (AFM) (Tyrrell and Attard, 2001, Holmberg et al., 2003, Steitz et al., 2003, Simonsen et al., 2004, Switkes and Ruberti, 2004, Agrawal et al., 2005, Zhang et al., 2006a, Zhang et al., 2006b and Zhang et al., 2006c). It has been shown that NBs at the liquid–solid interface resemble spherical caps with height and diameter of about 10 and 100 nm, respectively. In fact, this is supported by the fact that NBs can be fused by the tip of AFM to form a larger bubble (Simonsen et al., 2004). It was initially believed that NBs might have high surface tension, thus the gas should be ‘pressed out’ of NBs within microseconds after their formation (Matsumoto and Tanaka, 2008). However, NBs can form freely and remain stable for long periods of time under the right conditions. The stability of NBs results from a lower interfacial curvature than expected due to a high contact angle (Yang et al., 2003 and Zhang et al., 2006c). The formation of NBs in aqueous solutions of small organic molecules (e.g. tetrahydrofuran, ethanol, urea, and α -cyclodextrin) has also been reported (Jin et al., 2007a and Jin et al., 2007b).

Surface charge and bubble rising speed are vital factors for understanding the properties of MBs and NBs. It was found in an electrophoresis cell that MBs moved towards the oppositely charged electrode. The surface charge of each MB can be determined from the speed of its movement, which is correlated with the value of ζ potential (Yoon and Yordan, 1986, Everett, 1988, Li and Somasundaran, 1991, Graciaa et al., 2000, Kim et al., 2000 and Takahashi, 2005). In fact, due to the long stagnation of MBs, their ζ potential can be easily measured and in distilled water this is about -35 mV. It has been found that MBs are negatively charged under a wide range of pH. Although OH^- and H^+ ions have been shown to influence the charging mechanism of the gas–water interface (Takahashi, 2005). The ζ potential of the MBs has been found to be constant under similar water conditions irrespective of their size, indicating that the amount of electrical charge per unit area at the gas–water interface would remain constant (Takahashi, 2005). Nevertheless, increased ζ potential with the rate of shrinkage of MBs has been observed during collapse of

MBs (Fig. 2).

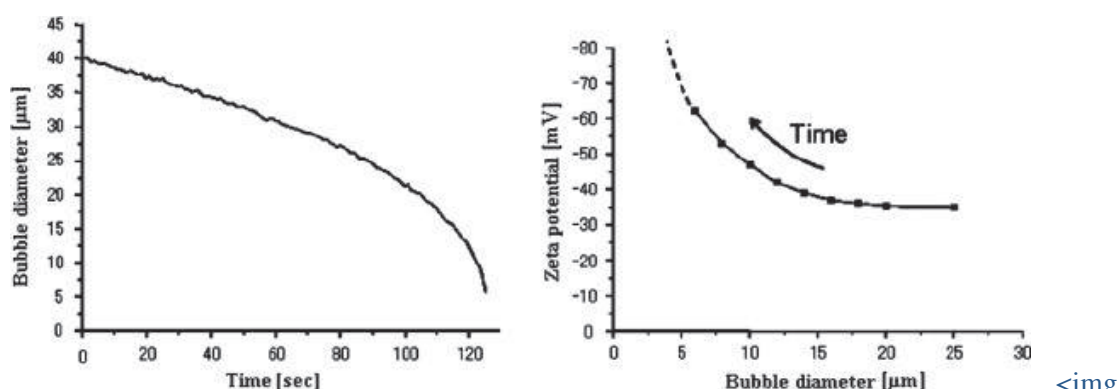


Fig. 2. Changes in the size and ζ potential of microbubbles over time (Takahashi et al., 2007b).

Figure options

Decrease in size of MBs below the water surface results in high internal pressure inside MBs, which is directly proportional to the bubble's diameter. The relationship between pressure and diameter is expressed by the Young–Laplace equation:

(1)

$$P = P_I + \frac{4\sigma}{d_b}$$

Comment

where P is the gas pressure, P_I is the liquid pressure, σ is the surface tension of the liquid and d_b is the bubble diameter. According to Henry's law, the amount of dissolved gas surrounding a shrinking bubble increases with the increase in gas pressure. The area surrounding a MB has been shown to change its state in a pressure–temperature (P – T) diagram to favor hydrate nucleation (Sloan, 1998). This is one of the typical characteristic of MBs.

3. Generation of free radicals by collapsing microbubbles in water

According to the Young–Laplace equation (Eq. (1)), for a bubble with diameter 1 μm at 298 K, the internal pressure is about 390 kPa, which is almost four times higher than the atmospheric pressure. Since the rate of increase in the internal pressure of MBs is inversely proportional to its size, a high pressure spot is eventually created at the final stage of the MB collapse (Fig. 3). If the collapsing speed of MBs is higher than the speed of sound in water, the temperature inside the collapsing bubbles may increase drastically due to adiabatic compression. Since the shrinkage rate of the collapsing bubbles is extremely slow compared to the ultrasonically induced cavitation bubbles, the temperature inside the collapsing MBs is likely much lower

than that inside the cavitation bubbles ($>5000\text{ K}$) (Takahashi et al., 2007a). Due to pyrolytic decomposition that takes place within the collapsing bubbles, the $\cdot\text{OH}$ radical and shock waves can be generated at the gas–liquid interface (Kimura and Ando, 2002). Since the rate of movement of electrolyte ions in water is not sufficiently high to counteract the increasing rate of shrinkage of the MBs, it is possible for some excess ions to be accumulated at the gas–water interface during the final stage of the collapse process which accounts for accelerated increase in the ζ potential (Takahashi et al., 2007b). As a result, the decomposition of ozone for producing $\cdot\text{OH}$ radicals would be expedited in case of ozone MBs (Takahashi et al., 2007a). The MBs of gases with oxidizing power (e.g. ozone) can be applied to various water treatment processes since the ozone MBs have high solubility and improved disinfection ability due to the generation of $\cdot\text{OH}$ radical and/or pressure waves (Sumikura et al., 2007).

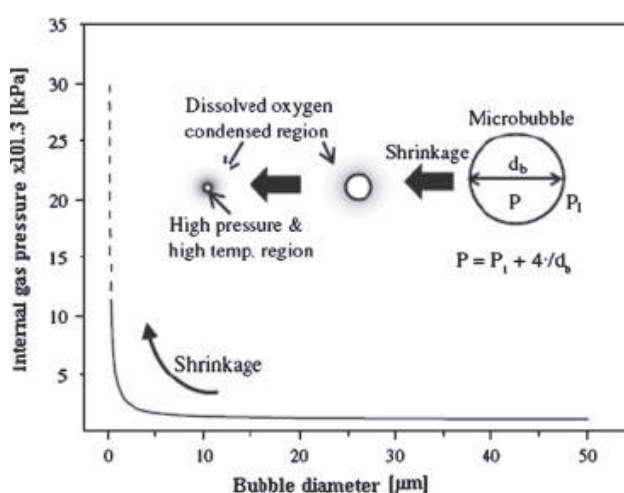


Fig. 3. Increase in the interior gas pressure of MBs during shrinkage (at $T=298\text{ K}$, $P = 100\text{ kPa}$.) (Li et al., 2009b).

caption

Figure options

Generation of free radicals through the collapse of MBs in the absence of dynamic stimulus has been experimentally demonstrated by electron spin resonance spectroscopy (Takahashi et al., 2007b). 5,5-dimethyl-1-pyrroline-N-oxide was chosen as the spin-trap agent to trap the free radicals generated in the process of collapse. The solution pH was found to have significant effect on the quantity of free radicals generated by the collapse of oxygen MBs, e.g. lowered pH enhanced generation of free radicals. Meanwhile, the type of gas used for the generation of MBs can also affect the quantity of free radicals generated. For example, oxygen MBs favored the formation of $\cdot\text{OH}$ radical compared to nitrogen MBs (Li et al., 2009a).

4. Methods for the generation of MBs and NBs

Formation, growth and collapse of MBs in solution is often referred to as cavitation.

Based on the mode of generation, cavitation is broadly classified into four categories, i.e. acoustic, hydrodynamic, optic and particle cavitation. The cavitation induced by the passage of ultrasonic waves is so-called acoustic cavitation, while cavitation due to the pressure variations in the flowing liquid is termed as hydrodynamic cavitation. Acoustic and hydrodynamic cavitations may result in the desired physical and chemical changes in a solution, but optic and particle cavitations are incapable of bringing about any change in the bulk solution.

Millions of hot spots in the reactor can be generated through hydrodynamic and acoustic cavitation due to very high localized energy density which in turn results in extremely high pressure and temperatures in the range of 10–500 MPa and 1000–10,000 K, respectively (Suslick, 1990). However, it should be noted that the collapse of MBs in the absence of dynamic stimulus would not favor the creation of such hot spots (Takahashi et al., 2007b). Nowadays, few methods have been developed for the generation of MBS and NBs. The two widely used methods are based on decompression and gas–water circulation. For the decompression type generator, a supersaturated condition for gas dissolution is created at high pressure of 304–405 kPa (Fig. 4). At such high pressure, supersaturated gas is highly unstable and eventually escapes out from the water. As the result, large number of MBs would be generated instantly. However, for gas–water circulation type generator, the gas is introduced into the water vortex, and gas bubbles are subsequently broken down into MBs by breaking up the vortex (Takahashi, 2009). Generation of the ozone MBs through decompression has been found to be more efficient than through gas–water circulation (Ikeura et al., 2011). Similar to the decompression type, the venturi-type MB generator has also been widely used. This has the advantages of compact size, low pump power and high-density generation of MBs normally with a mean diameter below 100 μm . The venturi-type generator consists of three main parts, i.e. inflow, tubule and tapered outflow. Cavitation occurs due to decrease in static pressure of the pressurized fluid entering the tubule part. In the tubule part, velocity of the fluid increases at the cost of decrease in static pressure. Simultaneously, gas entering into the tubule part from outside develops a multiphase-flow of the gas and liquid. When the fluid exceeds the speed of sound, a pressure wall with a shock wave is created in the tubule. MBs are thus generated through the collision of gas with the pressure wall developed with a shock wave (Yoshida et al., 2008).

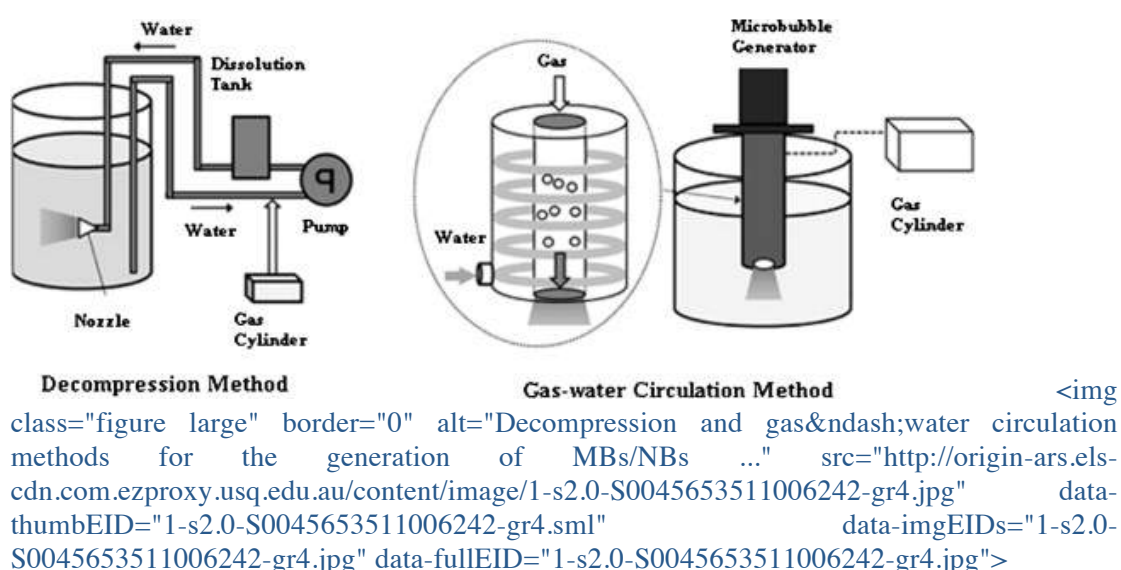


Fig. 4.

Decompression and gas–water circulation methods for the generation of MBs/NBs (Ikeura et al., 2011).

caption
Figure options

Besides the use of decompression and gas–water circulation methods for the generation of MBs, a palladium electrode coupled with ultrasonication has been used for generation of NBs with a mean diameter of 300–500 nm (Kim et al., 2000). Moreover, it has been reported that NBs with a mean diameter of 400–700 nm could be created by ultrasonication of a mixed surfactant solution with regular purging using octafluoropropane gas (Oeffinger and Wheatley, 2004). Lastly, it should be pointed out that generation of monodispersed MBs and NBs using the above methods still remain a major challenge.

5. Determination of bubble size

Laser diffraction particle size analyser has often been used to measure the size and size distribution of MBs and NBs (Kukizaki and Goto, 2006 and Tasaki et al., 2009b). The monodispersity of bubbles is determined according to the particle size dispersal coefficient δ :

equation

(2)

$$\delta = \frac{D_b^{90} - D_b^{10}}{D_b^{50}}$$

[View the MathML source](http://origin-ars.els-cdn.com.ezproxy.usq.edu.au/content/image/1-s2.0-S0045653511006242-si2.gif)

90

-Db10Db50

mathContainer Turn MathJax on Loading Mathjax

Comment

where D_b^{90} [View the MathML source](http://origin-ars.els-cdn.com.ezproxy.usq.edu.au/content/image/1-s2.0-S0045653511006242-si3.gif)

90

mathContainerLoading Mathjax, D_b^{50} [View the MathML source](http://origin-ars.els-cdn.com.ezproxy.usq.edu.au/content/image/1-s2.0-S0045653511006242-si4.gif)

50

mathContainerLoading Mathjax and D_b^{10} [View the MathML source](http://origin-ars.els-cdn.com.ezproxy.usq.edu.au/content/image/1-s2.0-S0045653511006242-si5.gif)

10

mathContainerLoading Mathjax are the diameters corresponding to 90%, 50%, and 10% by volume respectively, on the relative cumulative bubble size distribution

curve; D_b^{50} [View the MathML source](http://origin-ars.els-cdn.com.ezproxy.usq.edu.au/content/image/1-s2.0-S0045653511006242-si6.gif)

50

mathContainerLoading Mathjax represents the mean bubble diameter. The specific

interfacial area (a , $\text{m}^2 \text{m}^{-3}$) of MBs and NBs is defined by:
equation

(3)

$$a = \frac{6\varepsilon_G}{D_b^{50}}$$

6

$\varepsilon_G D_b$

50

mathContainer Turn MathJax on Loading Mathjax

Comment

equation

(4)

$$\varepsilon_G = \frac{V_G}{V_L + V_G}$$

$\varepsilon_G = V_G / (V_L + V_G)$
mathContainer Turn MathJax on Loading Mathjax

Comment

where ε_G is the gas holdup, V_G is the volume occupied by the gas phase (bubbles), V_L is the volume occupied by the liquid phase. The particle size can also be determined by scanning electron microscopy (SEM). For this purpose, a replica film had been developed (Ohgaki et al., 2010). Particle counting spectrometer for liquids which uses light-obscuration method can also be used for measuring the size distribution of MBs (Takahashi et al., 2003 and Takahashi et al., 2007a).

6. Water treatment by MBs and NBs technology

In the past few years, more and more attention has been given to the potential applications of the MBs and NBs for water treatment due to their ability to generate highly reactive free radicals. Recently, MBs/NBs have been used for detoxification of water (Yamasaki et al., 2010), while it has been reported that air and nitrogen MBs/NBs can enhance the activity of aerobic and anaerobic microorganisms in submerged membrane bioreactor. Evidence shows that nitrogen MBs/NBs cannot only be applied for water and wastewater treatment, but also for fermentation, brewing as well for human waste treatment. MBs/NBs have been found to catalyze chemical reactions, and enhance the detoxification efficiency, thereby improving the efficiency of chemical treatment of water. The main purpose of water pretreatment is to reduce biological, chemical and physical loads in order to reduce the running costs and increase the treated water quality. In this context, air MBs/NBs as a pretreatment means has been shown to be highly beneficial for downsizing the water/wastewater treatment plants and improving the quality of product water (Yamasaki et al., 2009 and Yamasaki et al., 2010).

6.1. Degradation of organic pollutants


MBs generated through hydrodynamic cavitation have been employed for degradation of various organic compounds, such as alachlor (Wang and Zhang, 2009), *p*-nitrophenol (Kalumuck and Chahine, 2000), rhodamine B (Wang et al., 2008) and decolorization of dye effluent stream (Sivakumar and Pandit, 2002).

Takahashi et al. (2007b) investigated the decomposition of phenol in aqueous solution with air MBs in the absence of dynamic stimulus (e.g. UV irradiation and incident ultrasonic wave). When 1.5 mM phenol solution was subjected to air MBs collapse for 3 h without addition of acid, no change in the phenol concentration was observed. However, 30% of phenol was decomposed after acid (e.g. nitric, sulfuric or hydrochloric acid) was added to the phenol solution, while intermediates, such as hydroquinone, benzoquinone, formic acid and oxalic acid were detected. Phenol could therefore be removed by free radicals generated through collapse of air MBs in the presence of a strong acid. The removal of polyvinyl alcohol (an ozone resistant) in terms of TOC by collapse of ozone MBs was also achieved under strong acidic conditions in the absence of dynamic stimulus (Takahashi et al., 2007a). As discussed earlier, the formation of hot spots by adiabatic compression of cavitation bubbles in an aggressive collapse process may further enhance organic degradation (Hart and Henglein, 1986). However, no reduction in TOC concentration confirmed that the hot spots generated by the ultrasound did not boost the generation of $\cdot\text{OH}$ radicals for the TOC removal. Excessive accumulation of ions around the gas–water interface of the collapsing MBs would lead to ion concentrations high enough for converting ozone to $\cdot\text{OH}$ radicals. The TOC reduction by ozone MBs under strong acidic conditions was much greater than using other conventional techniques. Ozonation of a mixture of benzene, toluene, ethylbenzene and xylenes had been reported at different salt concentrations ranging from 0 to 2 M (Walker et al., 2001). It was found that the production of MBs helped to improve the mass transfer efficiency and further enhanced the removal of soluble organics from simulated seawater.

Ozonation of synthetic wastewater containing azo dye and CI Reactive Black 5 was investigated using collapsing ozone MBs (Chu et al., 2007). In this experiment, the total mass transfer coefficient and pseudo-first order rate constant were found to be 1.8 and 3.2–3.6 times higher than those found in the bubble contractor, respectively. It was clearly shown that the production of $\cdot\text{OH}$ radicals was increased in the MB system. Evidence shows that the production of $\cdot\text{OH}$ radicals using vacuum UV irradiations (Oppenländer and Gliese, 2000) can lead to fast oxidation of organic compounds in water and wastewater as compared to the conventional ozone system without $\cdot\text{OH}$ radicals (Echigo et al., 1996). In addition, use of vacuum UV is restricted because of the recombination of carbon-centered radicals during photo degradation which yields undesirable byproducts, such as oligomers and polymers (Han et al., 2004). Recently, use of MBs and NBs technique to overcome the shortcomings of vacuum UV process has been explored (Tasaki et al., 2009a). Under vacuum UV irradiations the degradation of methyl orange in the presence of oxygen MBs was found to be accelerated due to the enhanced mass transfer of oxygen and substrate within the vacuum UV reactor (Tasaki et al., 2009b). The decolorization of methyl orange became faster under 185 + 254 nm irradiation with oxygen MBs. The critical role of NBs in degradation of surfactants and nonsurfactant under vacuum UV irradiations has also been investigated. The rate of mineralization of sodium dodecylbenzenesulfonate with 720 nm NBs was found to be much faster than that with MBs (Tasaki et al., 2009a). The observed enhanced mineralization of surfactants can be attributed to the high adsorption capacity of NBs due to their small size, and large specific surface area that facilitates the reaction.

6.2. Water disinfection

Generation of highly reactive free radicals and turbulence associated with the collapsing MBs provides great potential for water disinfection. Hydrodynamic cavitation has been shown to be a much cost-effective technique for water disinfection as compared to acoustic cavitation. However, lab-scale study suggests that the cost of hydrodynamic cavitation for water disinfection is still higher than conventional chlorination and ozonation (Jyoti and Pandit, 2001).

The effect of ozone MBs on *Escherichia coli* was investigated under various conditions. It has been found that the faster disinfection kinetics of *E. coli* by ozone MBs was observed, leading to a reduced reactor size and small ozone dose as compared to the conventional ozone disinfection for the same disinfection efficiency of a 2-log inactivation (Sumikura et al., 2007). In this process the  OH radical and shock waves generated by the collapse of MBs have been considered as the main cause for inactivation of coliform, while specific contribution of each effect to inactivation of coliform still remains unknown. Moreover, high deactivation efficiency of *E. coli* has also been achieved in water disinfection by MBs generated through hydrodynamic cavitation (Jyoti and Pandit, 2001, Jyoti and Pandit, 2003, Jyoti and Pandit, 2004, Arrojo et al., 2008 and Mezule et al., 2009). Bathing pool assembly having water full of ozone NBs for rehabilitation has also been developed to prevent pathogen growth (Chen, 2009). This assembly consists of a bath, a reservoir and two circulating systems. The circulating systems are connected to bath and reservoir via oxygen and ozone generator. Each circulating system is equipped with high pressure emulsifying device that facilitates generation of free radicals and anions from dissolved oxygen and ozone. The amount of ozone in the bath and the reservoir is maintained at the range of 0.5–5 and 0.2–0.5 mg L⁻¹, respectively. At a pressure of 304–1013 kPa provided by the high pressure emulsifying device, ozone is rapidly dissolved into water and ozone NBs in the range of 10–20 nm are thus produced. It was found that the subsequent burst of NBs would provide a more effective means for cleaning and disinfecting both the bath and the reservoir than traditional ultrasonic vibrator.

6.3. Cleaning and defouling of solid surfaces

NBs have been applied for the prevention and removal of proteins adsorbed onto solid surfaces. It has been shown that adsorption of proteins onto various surfaces could be inhibited by NBs, thus preventing the surfaces from fouling (Wu et al., 2006 and Wu et al., 2007). For example, NBs can block adsorption of bovine serum albumin on mica surface (Wu et al., 2006), while NBs also helps remove organic contaminants from pyrolytic graphite (Wu et al., 2007 and Wu et al., 2008) and gold surfaces (Liu et al., 2008). Recently, similar defouling effect of NBs was also observed on stainless steel surface (Chen, 2009).

The use of high frequency, low power ultrasound along with MBs has shown great potential in control of bacteria and algae attachment onto solid surfaces (Broekman et al., 2010). Destabilized and reduced biofilms have been observed after treatment by MBs. The bubble size has been found to affect the membrane fouling in case of tubular (Cui et al., 2003) and hollow fiber membranes (Lu et al., 2008 and Willems et al., 2009). (Tian et al., 2010) investigated the influence of mm sized air bubbles on membrane fouling of immersed hollow fiber membranes for ultrafiltration of river water, and found that continuous air bubbling would be more effective than intermittent bubbling in fouling control. In case of continuous bubbling, air bubbles scrub the membrane surface during the process of filtration and hence reduce the chances for the formation of concentration polarization and fouling layer on membrane surface. Moreover, it was observed that smaller air bubbles were more efficient in reducing fouling. In addition, similar phenomenon was also observed in other study of membrane fouling control by bubbling (Yeo et al., 2006, Van Kaam et

al., 2008, Zarragoitia-González et al., 2008 and Cornelissen et al., 2009).

7. Long-term perspectives of micro and nanobubbles technology

MBs and NBs have exhibited great potential in various engineering applications. For example, wide use of oxygen NBs has been anticipated due to their extremely high bioactivity and mass transfer efficiency. Due to their ability to generate free radicals without the use of any toxic chemical, MBs have been proven to be a new environmental friendly technique for oxidation of organic compounds, water disinfection and fouling control. It is reasonable to consider that MBs and NBs would have wide applications where materials come into contact with biological media, such as medical equipment, membrane cleaning, ship and filter regeneration. MBs and NBs may provide a promising path for a convenient, clean, cheap and environmental friendly technique suitable for cleaning of conducting surfaces. Hence, it can be concluded that the use of MBs and NBs in developing new technology is still ahead to be explored.

References

[Agrawal et al., 2005](#)

A. Agrawal, J. Park, D.Y. Ryu, P.T. Hammond, T.P. Russell, G.H. McKinley

Controlling the location and spatial extent of nanobubbles using hydrophobically nanopatterned surfaces

Nano Lett., 5 (2005), pp. 1751–1756

[Full Text via CrossRef](#) | [View Record in Scopus](#) | [Citing articles \(83\)](#)

[Arrojo et al., 2008](#)

S. Arrojo, Y. Benito, A. Martínez Tarifa

A parametrical study of disinfection with hydrodynamic cavitation

Ultrason. Sonochem., 15 (2008), pp. 903–908

[Article](#) | [Purchase PDF](#) | [View Record in Scopus](#) | [Citing articles \(35\)](#)

[Broekman et al., 2010](#)

S. Broekman, O. Pohlmann, E.S. Beardwood, E.C. de Meulenaer

Ultrasonic treatment for microbiological control of water systems

Ultrason. Sonochem., 17 (2010), pp. 1041–1048

[Article](#) | [Purchase PDF](#) | [View Record in Scopus](#) | [Citing articles \(42\)](#)

[Chen, 2009](#)

Chen, K.K., 2009. Bathing Pool Assembly with Water Full of Nano-Scale Ozone Bubbles for Rehabilitation. US Patent 7488416.

[Chu et al., 2007](#)

L.B. Chu, X.H. Xing, A.F. Yu, Y.N. Zhou, X.L. Sun, B. Jurcik

Enhanced ozonation of simulated dyestuff wastewater by microbubbles

Chemosphere, 68 (2007), pp. 1854–1860

[Article](#) | [Purchase PDF](#) | [View Record in Scopus](#) | [Citing articles \(64\)](#)

[Cornelissen et al., 2009](#)

E.R. Cornelissen, L. Rebour, D. van der Kooij, L.P. Wessels

Optimization of air/water cleaning (AWC) in spiral wound elements

Desalination, 236 (2009), pp. 266–272

[Article](#) | [Purchase PDF](#) | [View Record in Scopus](#) | [Citing articles \(11\)](#)

[Cui et al., 2003](#)

Z.F. Cui, S. Chang, A.G. Fane

The use of gas bubbling to enhance membrane processes

J. Membr. Sci., 221 (2003), pp. 1–35

[Article](#) | [Purchase PDF](#) | [View Record in Scopus](#) | [Citing articles \(280\)](#)
Echigo et al., 1996

S. Echigo, H. Yamada, S. Matsui, S. Kawanishi, K. Shishida
Comparison between O_3 /VUV, O_3/H_2O_2 , VUV and O_3 processes for the decomposition of organophosphoric acid triesters
Water Sci. Technol., 34 (9) (1996), pp. 81–88

[Article](#) | [Purchase PDF](#) | [View Record in Scopus](#) | [Citing articles \(48\)](#)
Eriksson and Ljunggren, 1999

J.C. Eriksson, S. Ljunggren
On the mechanically unstable free energy minimum of a gas bubble which is submerged in water and adheres to a hydrophobic wall

Colloid Surf. A, 159 (1999), pp. 159–163

[Article](#) | [Purchase PDF](#) | [View Record in Scopus](#) | [Citing articles \(25\)](#)
Everett, 1988

D.H. Everett

Basic Principles of Colloid Science

Royal Society of Chemistry, London (1988)

[Graciaa et al., 2000](#)

A. Graciaa, P. Creux, J. Lachaise, J.L. Salager

ζ Potential at an air–water surface related to the critical micelle concentration of aqueous mixed surfactant systems

Ind. Eng. Chem. Res., 39 (2000), pp. 2677–2681

[Full Text via CrossRef](#) | [View Record in Scopus](#) | [Citing articles \(10\)](#)

[Han et al., 2004](#)

W. Han, P. Zhang, W. Zhu, J. Yin, L. Li

Photocatalysis of p-chlorobenzoic acid in aqueous solution under irradiation of 254 nm and 185 nm UV light

Water Res., 38 (2004), pp. 4197–4203

[Article](#) | [Purchase PDF](#) | [View Record in Scopus](#) | [Citing articles \(45\)](#)

Hart and Henglein, 1986

E.J. Hart, A. Henglein

Sonolysis of ozone in aqueous solution

J. Phys. Chem., 90 (1986), pp. 3061–3062

[Full Text via CrossRef](#) | [View Record in Scopus](#) | [Citing articles \(34\)](#)

[Holmberg et al., 2003](#)

M. Holmberg, A. Kühle, J. Garnæs, K.A. Mørch, A. Boisen

Nanobubble trouble on gold surfaces

Langmuir, 19 (2003), pp. 10510–10513

[Full Text via CrossRef](#) | [View Record in Scopus](#) | [Citing articles \(113\)](#)

[Ikeura et al., 2011](#)

H. Ikeura, F. Kobayashi, M. Tamaki

Removal of residual pesticide, fenitrothion, in vegetables by using ozone microbubbles generated by different methods

J. Food Eng., 103 (2011), pp. 345–349

[Article](#) | [Purchase PDF](#) | [View Record in Scopus](#) | [Citing articles \(29\)](#)

[Jin et al., 2007a](#)

F. Jin, J. Li, X. Ye, C. Wu

Effects of pH and ionic strength on the stability of nanobubbles in aqueous solutions of α -cyclodextrin

J. Phys. Chem. B, 111 (2007), pp. 11745–11749

[Full Text via CrossRef](#) | [View Record in Scopus](#) | [Citing articles \(48\)](#)

[Jin et al., 2007b](#)

F. Jin, X. Ye, C. Wu

Observation of kinetic and structural scalings during slow coalescence of nanobubbles in an aqueous solution

J. Phys. Chem. B, 111 (2007), pp. 13143–13146

[Full Text via CrossRef](#) | [View Record in Scopus](#) | [Citing articles \(22\)](#)

[Jyoti and Pandit, 2001](#)

K.K. Jyoti, A.B. Pandit

Water disinfection by acoustic and hydrodynamic cavitation

Biochem. Eng. J., 7 (2001), pp. 201–212

[Article](#) | [Purchase PDF](#) | [View Record in Scopus](#) | [Citing articles \(69\)](#)

[Jyoti and Pandit, 2003](#)

K.K. Jyoti, A.B. Pandit

Hybrid cavitation methods for water disinfection: simultaneous use of chemicals with cavitation

Ultrason. Sonochem., 10 (2003), pp. 255–264

[Article](#) | [Purchase PDF](#) | [View Record in Scopus](#) | [Citing articles \(42\)](#)

[Jyoti and Pandit, 2004](#)

K.K. Jyoti, A.B. Pandit

Ozone and cavitation for water disinfection

Biochem. Eng. J., 18 (2004), pp. 9–19

[Article](#) | [Purchase PDF](#) | [View Record in Scopus](#) | [Citing articles \(56\)](#)

VALIDHTML

[Kalumuck and Chahine, 2000](#)

K.M. Kalumuck, G.L. Chahine

The use of cavitating jets to oxidize organic compounds in water

J. Fluid. Eng. T. ASME, 122 (2000), pp. 465–470

[Full Text via CrossRef](#) | [View Record in Scopus](#) | [Citing articles \(70\)](#)

[Kim et al., 2000](#)

J.Y. Kim, M.G. Song, J.D. Kim

Zeta potential of nanobubbles generated by ultrasonication in aqueous alkyl polyglycoside solutions

J. Colloid Interface Sci., 223 (2000), pp. 285–291

[Article](#) | [Purchase PDF](#) | [View Record in Scopus](#) | [Citing articles \(55\)](#)

[Kimura and Ando, 2002](#)

T. Kimura, T. Ando

Physical control of chemical reaction by ultrasonic waves

Ultrason. Technol., 14 (2002), pp. 7–8

[View Record in Scopus](#) | [Citing articles \(4\)](#)

[Kukizaki and Goto, 2006](#)

M. Kukizaki, M. Goto

Size control of nanobubbles generated from Shirasu-porous-glass (SPG) membranes

J. Membr. Sci., 281 (2006), pp. 386–396

[Article](#) | [Purchase PDF](#) | [View Record in Scopus](#) | [Citing articles \(62\)](#)

[Li and Somasundaran, 1991](#)

C. Li, P. Somasundaran

Reversal of bubble charge in multivalent inorganic salt solutions – effect of magnesium

J. Colloid Interface Sci., 146 (1991), pp. 215–218

[Article](#) | [Purchase PDF](#) | [View Record in Scopus](#) | [Citing articles \(120\)](#)

[Li et al., 2009a](#)

P. Li, M. Takahashi, K. Chiba

Degradation of phenol by the collapse of microbubbles

Chemosphere, 75 (2009), pp. 1371–1375

[Article](#) | [Purchase PDF](#) | [View Record in Scopus](#) | [Citing articles \(34\)](#)

[Li et al., 2009b](#)

P. Li, M. Takahashi, K. Chiba

Enhanced free-radical generation by shrinking microbubbles using a copper catalyst

Chemosphere, 77 (2009), pp. 1157–1160

[Article](#) | [Purchase PDF](#) | [View Record in Scopus](#) | [Citing articles \(37\)](#)

[Liu et al., 2008](#)

G. Liu, Z. Wu, V.S.J. Craig

Cleaning of protein-coated surfaces using nanobubbles: an investigation using a Quartz Crystal Microbalance

J. Phys. Chem. C, 112 (2008), pp. 16748–16753

[Full Text via CrossRef](#) | [View Record in Scopus](#) | [Citing articles \(39\)](#)

[Ljunggren and Eriksson, 1997](#)

S. Ljunggren, J.C. Eriksson

The lifetime of a colloid-sized gas bubble in water and the cause of the hydrophobic attraction

Colloid. Surf. A, 129–130 (1997), pp. 151–155

[Article](#) | [Purchase PDF](#) | [View Record in Scopus](#) | [Citing articles \(137\)](#)

[Lu et al., 2008](#)

Y. Lu, Z. Ding, L. Liu, Z. Wang, R. Ma

The influence of bubble characteristics on the performance of submerged hollow fiber membrane module used in microfiltration

Sep. Purif. Technol., 61 (2008), pp. 89–95

[Article](#) | [Purchase PDF](#) | [View Record in Scopus](#) | [Citing articles \(26\)](#)

[Matsumoto and Tanaka, 2008](#)

M. Matsumoto, K. Tanaka

Nano bubble-Size dependence of surface tension and inside pressure

Fluid Dyn. Res., 40 (2008), pp. 546–553

[Article](#) | [Purchase PDF](#) | [Full Text via CrossRef](#) | [View Record in Scopus](#) | [Citing articles \(51\)](#)

[Mezule et al., 2009](#)

L. Mezule, S. Tsyfansky, V. Yakushevich, T. Juhna

A simple technique for water disinfection with hydrodynamic cavitation: effect on survival of *Escherichia coli*

Desalination, 248 (2009), pp. 152–159

[Article](#) | [Purchase PDF](#) | [View Record in Scopus](#) | [Citing articles \(19\)](#)

[Oeffinger and Wheatley, 2004](#)

B.E. Oeffinger, M.A. Wheatley

Development and characterization of a nano-scale contrast agent

Ultrasonics, 42 (2004), pp. 343–347

[Article](#) | [Purchase PDF](#) | [View Record in Scopus](#) | [Citing articles \(91\)](#)

[Ohgaki et al., 2010](#)

K. Ohgaki, N.Q. Khanh, Y. Joden, A. Tsuji, T. Nakagawa

Physicochemical approach to nanobubble solutions

Chem. Eng. Sci., 65 (2010), pp. 1296–1300

[Article](#) | [Purchase PDF](#) | [View Record in Scopus](#) | [Citing articles \(56\)](#)

[Oppenländer and Gliese, 2000](#)

T. Oppenländer, S. Gliese

Mineralization of organic micropollutants (homologous alcohols and phenols) in water by vacuum-UV-oxidation (H₂O-VUV) with an incoherent xenon-excimer lamp at 172 nm

Chemosphere, 40 (2000), pp. 15–21

[Article](#) | [Purchase PDF](#) | [View Record in Scopus](#) | [Citing articles \(41\)](#)

[Simonsen et al., 2004](#)

A.C. Simonsen, P.L. Hansen, B. Klösgen

Nanobubbles give evidence of incomplete wetting at a hydrophobic interface

J. Colloid Interface Sci., 273 (2004), pp. 291–299

[Article](#) | [Purchase PDF](#) | [View Record in Scopus](#) | [Citing articles \(132\)](#)

[Sivakumar and Pandit, 2002](#)

M. Sivakumar, A.B. Pandit

Wastewater treatment: a novel energy efficient hydrodynamic cavitation technique

Ultrason. Sonochem., 9 (2002), pp. 123–131

[Article](#) | [Purchase PDF](#) | [View Record in Scopus](#) | [Citing articles \(111\)](#)

[Sloan, 1998](#)

E.D. Sloan Jr.

Gas hydrates: review of physical/chemical properties

Energy Fuels, 12 (1998), pp. 191–196

[Full Text via CrossRef](#) | [View Record in Scopus](#) | [Citing articles \(102\)](#)

[Steitz et al., 2003](#)

R. Steitz, T. Gutberlet, T. Hauss, B. Klösgen, R. Krastev, S.

Schemmel, A.C. Simonsen, G.H. Findenegg

Nanobubbles and their precursor layer at the interface of water against a hydrophobic substrate

Langmuir, 19 (2003), pp. 2409–2418

[Full Text via CrossRef](#) | [View Record in Scopus](#) | [Citing articles \(256\)](#)

[Sumikura et al., 2007](#)

M. Sumikura, M. Hidaka, H. Murakami, Y. Nobutomo, T. Murakami

Ozone micro-bubble disinfection method for wastewater reuse system

Water Sci. Technol., 56 (5) (2007), pp. 53–61

[Full Text via CrossRef](#) | [View Record in Scopus](#) | [Citing articles \(27\)](#)

VALIDHTML

[Suslick, 1990](#)

K.S. Suslick

Sonochemistry

Science, 247 (1990), pp. 1439–1445

[Loading](#)

[Switkes and Ruberti, 2004](#)

M. Switkes, J.W. Ruberti

Rapid cryofixation/freeze fracture for the study of nanobubbles at solid–liquid interfaces

Appl. Phys. Lett., 84 (2004), pp. 4759–4761

[Loading](#)

[Takahashi, 2005](#)

M. Takahashi

ζ Potential of microbubbles in aqueous solutions: electrical properties of the gas–water interface

J. Phys. Chem. B, 109 (2005), pp. 21858–21864

[Loading](#)

[Takahashi, 2009](#)

M. Takahashi

Base and technological application of micro-bubble and nanobubble

Mater. Integration, 22 (2009), pp. 2–19

[Loading](#)

[Takahashi et al., 2007a](#)

M. Takahashi, K. Chiba, P. Li

Formation of hydroxyl radicals by collapsing ozone microbubbles under strongly acidic conditions

J. Phys. Chem. B, 111 (2007), pp. 11443–11446

Loading

[Takahashi et al., 2007b](#)

M. Takahashi, K. Chiba, P. Li

Free-radical generation from collapsing microbubbles in the absence of a dynamic stimulus

J. Phys. Chem. B, 111 (2007), pp. 1343–1347

Loading

[Takahashi et al., 2003](#)

M. Takahashi, T. Kawamura, Y. Yamamoto, H. Ohnari, S. Himuro, H. Shakutsui

Effect of shrinking microbubble on gas hydrate formation

J. Phys. Chem. B, 107 (2003), pp. 2171–2173

Loading

[Tasaki et al., 2009a](#)

T. Tasaki, T. Wada, Y. Baba, M. Kukizaki

Degradation of surfactants by an integrated nanobubbles/vuv irradiation technique

Ind. Eng. Chem. Res., 48 (2009), pp. 4237–4244

Loading

[Tasaki et al., 2009b](#)

T. Tasaki, T. Wada, K. Fujimoto, S. Kai, K. Ohe, T. Oshima, Y. Baba, M. Kukizaki

Degradation of methyl orange using short-wavelength UV irradiation with oxygen microbubbles

J. Hazard. Mater., 162 (2009), pp. 1103–1110

Loading

[Tian et al., 2010](#)

J.Y. Tian, Y.P. Xu, Z.L. Chen, J. Nan, G.B. Li

Air bubbling for alleviating membrane fouling of immersed hollow-ber membrane for ultrafiltration of river water

Desalination, 260 (2010), pp. 225–230

Loading

[Tyrrell and Attard, 2001](#)

J.W.G. Tyrrell, P. Attard

Images of nanobubbles on hydrophobic surfaces and their interactions

Phys. Rev. Lett., 87 (2001), pp. 1761041–1761044

Loading

[Van Kaam et al., 2008](#)

R. Van Kaam, D. Anne-Archard, M.A. Gaubert, C. Albasi

Rheological characterization of mixed liquor in a submerged membrane bioreactor: interest for process management

J. Membr. Sci., 317 (2008), pp. 26–33

Loading

[Walker et al., 2001](#)

A.B. Walker, C. Tsouris, D.W. DePaoli, K.T. Klasson

Ozonation of soluble organics in aqueous solutions using microbubbles

Ozone Sci. Eng., 23 (2001), pp. 77–87

Loading

[Wang et al., 2008](#)

X. Wang, J. Wang, P. Guo, W. Guo, G. Li

Chemical effect of swirling jet-induced cavitation: degradation of rhodamine B in aqueous solution

Ultrason. Sonochem., 15 (2008), pp. 357–363

Loading

[Wang and Zhang, 2009](#)

X. Wang, Y. Zhang

Degradation of alachlor in aqueous solution by using hydrodynamic cavitation

J. Hazard. Mater., 161 (2009), pp. 202–207

Loading

[Willems et al., 2009](#)

P. Willems, A.J.B. Kemperman, R.G.H. Lammertink, M. Wessling, M. van Sint Annaland, N.G. Deen, J.A.M. Kuipers, W.G.J. van der Meer

Bubbles in spacers: direct observation of bubble behavior in spacer filled membrane channels

J. Membr. Sci., 333 (2009), pp. 38–44

Loading

[Wu et al., 2006](#)

Z. Wu, X. Zhang, G. Li, J. Sun, Y. Zhang, M. Li, J. Hu

Nanobubbles influence on BSA adsorption on mica surface

Surf. Interface Anal., 38 (2006), pp. 990–995

Loading

[Wu et al., 2007](#)

Z. Wu, X. Zhang, J. Sun, Y. Dong, J. Hu

In situ AFM observation of BSA adsorption on HOPG with nanobubble

Chin. Sci. Bull., 52 (2007), pp. 1913–1919

Loading

[Wu et al., 2008](#)

Z.H. Wu, H.B. Chen, Y.M. Dong, H.L. Mao, J.L. Sun, S.F. Chen, V.S.J. Craig, J. Hu

Cleaning using nanobubbles: defouling by electrochemical generation of bubbles

J. Colloid Interface Sci., 328 (2008), pp. 10–14

Loading

[Yamasaki et al., 2010](#)

Yamasaki, K., Sakata, K., Chuhjoh, K., 2010. Water Treatment Method and Water Treatment System. US Patent 7662288.

Loading

VALIDHTML

[Yamasaki et al., 2009](#)

Yamasaki, K., Uda, K., Chuhjoh, K., 2009. Wastewater Treatment Equipment and Method of Wastewater Treatment. US Patent 7578942 B2.

Loading

[Yang et al., 2003](#)

J. Yang, J. Duan, D. Fornasiero, J. Ralston

Very small bubble formation at the solid–water interface

J. Phys. Chem. B, 107 (2003), pp. 6139–6147

Loading

[Yeo et al., 2006](#)

A.P.S. Yeo, A.W.K. Law, A.G. Fane

Factors affecting the performance of a submerged hollow fiber

bundle

J. Membr. Sci., 280 (2006), pp. 969–982

Loading

[Yoon and Yordan, 1986](#)

R.H. Yoon, J.L. Yordan

Zeta-potential measurements on microbubbles generated using various surfactants

J. Colloid Interface Sci., 113 (1986), pp. 430–438

Loading

[Yoshida et al., 2008](#)

A. Yoshida, O. Takahashi, Y. Ishii, Y. Sekimoto, Y. Kurata

Water purification using the adsorption characteristics of microbubbles

Jpn. J. Appl. Phys., 47 (2008), pp. 6574–6577

Loading

[Zarragoitia-González et al., 2008](#)

A. Zarragoitia-González, S. Schetrite, M. Alliet, U. Jáuregui-Haza, C. Albasi

Modelling of submerged membrane bioreactor: conceptual study about link between activated sludge biokinetics, aeration and fouling process

J. Membr. Sci., 325 (2008), pp. 612–624

Loading

[Zhang et al., 2006a](#)

L. Zhang, Y. Zhang, X. Zhang, Z. Li, G. Shen, M. Ye, C. Fan, H. Fang, J. Hu

Electrochemically controlled formation and growth of hydrogen nanobubbles

Langmuir, 22 (2006), pp. 8109–8113

Loading

[Zhang et al., 2006b](#)

X.H. Zhang, G. Li, N. Maeda, J. Hu

Removal of induced nanobubbles from water/graphite interfaces by partial degassing

Langmuir, 22 (2006), pp. 9238–9243

Loading

[Zhang et al., 2006c](#)

X.H. Zhang, N. Maeda, V.S.J. Craig

Physical properties of nanobubbles on hydrophobic surfaces in water and aqueous solutions

Langmuir, 22 (2006), pp. 5025–5035

Loading

Corresponding author. Tel.: +65 67905254; fax: +65 67910676.

footerNotes

Copyright © 2011 Elsevier Ltd. All rights reserved.



(07) 3118 5927

info@solariwater.com.au

www.solariwater.com.au

477 Boundary Street,
Spring Hill QLD 4000